Interplay between shape and magnetocrystalline anisotropies in patterned bcc Fe/Co(001) multilayers

O. Kazakova*
Department of Solid State Physics, Chalmers University of Technology and Göteborg University, SE-412 96 Göteborg, Sweden
and National Physical Laboratory, Teddington TW11 0LW, United Kingdom

M. Hanson
Department of Solid State Physics, Chalmers University of Technology and Göteborg University, SE-412 96 Göteborg, Sweden

P. Blomqvist and R. Wäppling
Department of Physics, Uppsala University, Box 530, SE-751 21 Uppsala, Sweden
(Received 15 October 2002; revised manuscript received 21 February 2003; published 15 March 2004)

In this work the interplay between magnetocrystalline and shape anisotropies was studied in submicron size particles made of bcc Fe/Co(001) multilayers of thickness 20 nm and Co content in the range 27–75 at. %. Arrays of circular and elliptical particles with well-defined geometry and lateral sizes in the range 150–550 nm were prepared by electron-beam lithography and ion milling and investigated by magnetization measurements and magnetic force microscopy (MFM). The angular dependence of the magnetization of the initial films demonstrates the change of the easy direction of magnetization (in plane) from [100] to [110] as one goes from pure Fe to Fe/Co multilayers with increasing Co content. The first-order anisotropy constant K_1 is negative for the investigated Fe/Co films and depends linearly on the Co concentration. By extrapolation, the change of sign is obtained at about 23 at. % of Co. The high effective magnetic moment of the multilayers, up to $(2.8 \pm 0.3)\mu_B$ per atom for the Fe2/Co6 multilayer film, may be explained by an enhancement of the local moments both on Fe and Co and a spin dependent polarization of the electron gas, due to confinement in the individual (0.3–1.2 nm thick) Fe and Co layers. The domain structure and magnetization reversal processes of circular particles (diameter 550 nm) are governed by the shape anisotropy for the nearly isotropic Fe8/Co3 multilayers and by the high magnetocrystalline anisotropy in Fe2/Co6 multilayers. The MFM investigation of elliptical particles with aspect ratio 1:3 reveals that only in the case with cooperating shape and strong magnetocrystalline anisotropies a stable single domain state is formed in the majority (78%) of the elements. From magnetization measurements we deduce that the elliptical particles are in quasisingle domain states (so called *C* and *S* states) during magnetization reversal.

DOI: 10.1103/PhysRevB.69.094408 PACS number(s): 75.60.−d, 75.70.−i, 75.75.+a

I. INTRODUCTION

Thin magnetic films and, in particular, submicron structures made of them attract interest both for technical applications and fundamental research. Magnetic multilayers and alloys containing $3d$-transition metals are being especially extensively investigated. Since the magnetic properties of a material strongly depend on its microstructure, crystallographic modifications can be used as a tool for tuning of the magnetic properties. It is well known that metastable structural phases can be stabilized on suitable substrates. For example, cobalt which has an hcp equilibrium structure, can be grown as a bcc thin film by molecular-beam epitaxy (MBE) on GaAs substrates.[1] Another possibility is to grow bcc Co by epitaxial stabilization of this phase in a bcc Fe/Co superlattice on GaAs by MBE (Refs. 2,3) or on MgO substrates either by MBE or dc magnetron sputtering.[4–7] A considerable amount of theoretical as well as experimental work on bcc Co films and Fe/Co multilayers has been motivated by their great importance for understanding the magnetism of surfaces and interfaces. It was predicted already in 1954 by Néel[8] that the reduced symmetry at a surface may cause an increase of the magnetic anisotropy energy, as compared to that of bulk materials. Furthermore, it is of interest to study the effective magnetic moments of the $3d$-transition metals, which are known to be sensitive to the local atomic environment. FeCo alloys with bcc structure showed extreme magnetic properties, e.g., high Curie temperature and high saturation magnetization.[9] Polarized neutron-diffraction studies[10] and electron energy-loss spectroscopy[11] yielded an increase of the magnetic moment of Fe from $2.2\mu_B$ per atom in pure Fe to $3.0\mu_B$ per Fe atom in bcc alloys with 30–70 at. % Co. While in FeCo alloys the concentration dependence of the magnetization was investigated, taking into account the ordering-disordering processes in alloys, in bcc Fe/Co multilayers one has a chance to study this dependence with each component being localized in a layer (provided the interface between Fe and Co is sharp). In bcc Fe/Co multilayers, magnetization[12] and magnetic circular x-ray dichroism (MCXD) (Ref. 13) measurements indicate that the magnetic moment of Fe is considerably enhanced, up to $3.0\mu_B$ per Fe atom close to interfaces, but recovering the bulk value away from the interface. A Mössbauer study of a Fe/Co superlattice[14] showed, however, a maximum increase of

about 13% of the magnetic hyperfine field at the iron nuclei, which would yield a magnetic moment of only $2.5\mu_B$ for iron using the ''normal'' conversion factor between hyperfine fields and magnetic moment. In many of the studies it was concluded that the moment of Co changes little ($1.65–1.83\mu_B$) with composition both in alloys and multilayers, in experiments[10,13] as well as theory.[15–18] However, to explain the observed values of the saturation magnetization in bcc Fe/Co (001) superlattices it was assumed that the Co moment can be enhanced up to $2.1\mu_B$ per atom close to interfaces.[19] Co-coated Fe clusters is another interesting magnetic material, in which enhancement in both the spin and orbital magnetic moments of Fe was deduced theoretically[20] and observed experimentally by MCXD.[21,22] The effects were found to depend on cluster morphology and size.

In spite of the large amount of work devoted to studies of alloy films and multilayers of Fe and Co, only a few deal with patterned structures[23,24] prepared of these materials. At the same time, patterned structures containing Fe, Co, or FeCo layers are gaining increasing interest as elements in magnetoelectronic devices, e.g., MRAM cells and read heads.[25,26] Patterned structures also allow studies of fundamental magnetic phenomena such as the processes of magnetization reversal, the formation of domain structures, and their dependence on the particle geometry (size and shape), interactions (distance between particles and their shape) as well as on intrinsic properties of the material (magnetocrystalline anisotropy and atomic magnetic moment). This motivated us to make an investigation of patterned Fe/Co multilayers with varying Co concentrations.

In our previous studies[27,28] we studied the influence of shape anisotropy and effects of dipolar interactions on both the domain structure and the processes of magnetization reversal in patterned Fe/Co multilayers containing 75 at. % of Co. Here we focus our attention on the interplay between the magnetocrystalline and shape anisotropies. In the design of a submicron size element for a particular application, one must control both the intrinsic magnetic properties determined by the material parameters of the film and the shape of the element which modifies the magnetostatic energy of the element. Choosing epitaxial multilayers with different combinations of Fe and Co monolayers yields an excellent opportunity to tune the strength and orientation of the magnetocrystalline energy of the system.[19] Furthermore, this can be accomplished while preserving the crystal structure and a ferromagnetic coupling between the layers as well as keeping the values of the saturation magnetization within a narrow range. By patterning the film the shape anisotropy of the layered structures is changed, and thereby the relation between the two components of magnetic anisotropy can be varied. In this paper we present an investigation, by magnetization measurements and atomic and magnetic force microscopy (AFM/MFM), of four combinations of Fe/Co multilayers with total film thicknesses of about 20 nm. The films are patterned to yield particles of circular and elliptical shape with lateral dimensions in the range 150–550 nm. The results are interpreted in terms of the changing magnetocrystalline anisotropy in the starting materials, as the composition of the multilayers varies between pure Fe (Refs. 29,30) and Co.[31]

II. EXPERIMENTAL METHODS

A. Sample preparation

The Fe/Co multilayers were grown on MgO substrates in a three target magnetron sputtering system under identical conditions as for another set of Fe/Co multilayers.[7] The structure of those films was extensively studied, and we consider the present films to have the same crystal structure and epitaxial relationships: bcc with lattice constants 2.866 Å and 2.828 Å for the Fe and Co layers, respectively, where Fe/Co [001] || MgO [001] and Fe/Co [110] || MgO [100]. Four films comprising layers with the following numbers of Fe and Co monolayers and atomic concentrations of Co were prepared: Fe8/Co3 (27%), Fe7/Co3 (30%), Fe4/Co2 (33%), and Fe2/Co6 (75%). The number of repetitions was chosen in each case to keep the thickness of the samples constant ($t \approx 20$ nm). The multilayers were capped by a thin layer of V to avoid oxidation. The film thickness was determined from the deposition rate during preparation. Since this yields an accuracy of the absolute value within 2 nm, the thickness was determined also from AFM on the patterned samples. The agreement between the two methods was within 1 nm, except for Fe4/Co2 where AFM implied a 5 nm thicker film than the deposition rate.

The magnetic particles were fabricated by a combination of electron-beam lithography and ion milling using a double-layered resist, a carbon masking layer, and a NiCr layer for pattern transfer, in a way similar to that described earlier.[32] The sets of particles with different sizes and shapes were prepared over regions of 2.5 mm$\times$2.5 mm within a total area of 10 mm$\times$10 mm. Each sample thus contains 10^7–10^8 particles. Particles of circular shape, designed as octagons with diameters $d_c = 200$ and 550 nm, were positioned in a square lattice with lattice constants 1200 and 1100 nm respectively. The lattice axes were oriented along the [100] and [010] MgO directions. Particles of elliptical shape were made with long and short axes $l = 450$ nm and $s = 150$ nm and lattice constants $a_l = 900$ nm and $b_s = 1150$ nm, respectively. The elliptical particles were positioned in two different rectangular arrays with the long axis along either the [100] or the [110] MgO direction. Reference samples of circular shape with diameter 1.7 mm were prepared in the same process for each of the Fe/Co films. The lithography and the milling process yield patterns with well-defined shape and lateral extension,[29] as verified by scanning electron microscopy (SEM) and atomic force microscopy (AFM). For magnetic measurements the wafers were finally diced into rectangular samples using a diamond saw.

B. Magnetic characterization.

The macroscopic magnetization was measured using an alternating gradient magnetometer (AGM). All samples were investigated at room temperature in magnetic fields B in the range $-2\ \mathrm{T} < B < 2\ \mathrm{T}$, applied in different directions in the plane of the film. The reference samples were further

checked for out-of-plane components of magnetization. In order to avoid spurious effects in the magnetization curves, the measurements were carried out with an amplitude of the alternating gradient field well below the coercivity field. The hysteresis curves were corrected for the diamagnetic background of the substrate and sample holder, whereafter the coercivity B_c and the saturation and remanent magnetic moments m_s and m_r of the sample were determined. The saturation magnetization M_s and the saturation remanent magnetization M_r were obtained by dividing m_s and m_r by the volume of the magnetic material in each sample. The topography and the local distribution of magnetic moments of the individual particles were studied by an AFM/MFM scanning probe technique using a Dimension^{TM} 3000 microscope from Digital Instruments (DI). Images were obtained with the instrument operated in the tapping and lift modes using the standard MFM tips supplied by DI. The tips were magnetized in the direction normal to the sample. The MFM measurements were performed on the samples in the as-grown state and after different magnetic-field histories, e.g., ac demagnetization.

III. RESULTS

A. Fe/Co continuous films

The results of the magnetization measurements with the field applied in the [100] and [110] directions of the bcc Fe/Co reference samples are presented in Fig. 1 for fields in the ranges ± 0.1 T (left column) and ± 0.01 T (right column). Hysteresis curves for a pure bcc Fe(001) film of the same thickness ($t=20$ nm) are shown for comparison. The curves show the archetypal behavior of thin bcc Fe(001) films where the bulk hard direction [111] is not present in the plane of the film. This leads to a cubic in-plane magnetocrystalline anisotropy with easy and hard axes along the [100] and [110] directions, respectively. As the Co layers are introduced into the Fe lattice the magnetic anisotropy first decreases and then a redistribution of the magnetocrystalline axes occurs: [110] becomes the easy and [100] the hard direction of magnetization. In the Fe8/Co3 multilayer film, with the minimum Co content 27%, a small difference between the [100] and [110] directions can be seen only in low fields, below 3 mT. Otherwise this film is nearly isotropic. A more pronounced difference between the easy [110] and hard [100] directions is observed as the Co content increases to 30% in Fe7/Co3. The two films with 33% and 75% Co (Fe4/Co2 and Fe2/Co6) are further characterized by the higher field required to close the hysteresis loops. All multilayers show a fourfold in-plane anisotropy with no indication of a uniaxial component. The first-order anisotropy constant K_1 was estimated from the area between the hysteresis curves measured in the [110] and [100] directions.[33] This analysis yields $K_1=-3.0$ kJm^{-3}, -13.6 kJm^{-3}, -30.0 kJm^{-3}, and -75.3 kJm^{-3} for the Co concentrations 27%, 30%, 33%, and 75%, respectively (see also Table I).

The magnitude of K_1 depends almost linearly on the Co concentration in the range 27–75% and a linear extrapolation of the values yields $K_1=0$ for a Co content of about 23%.

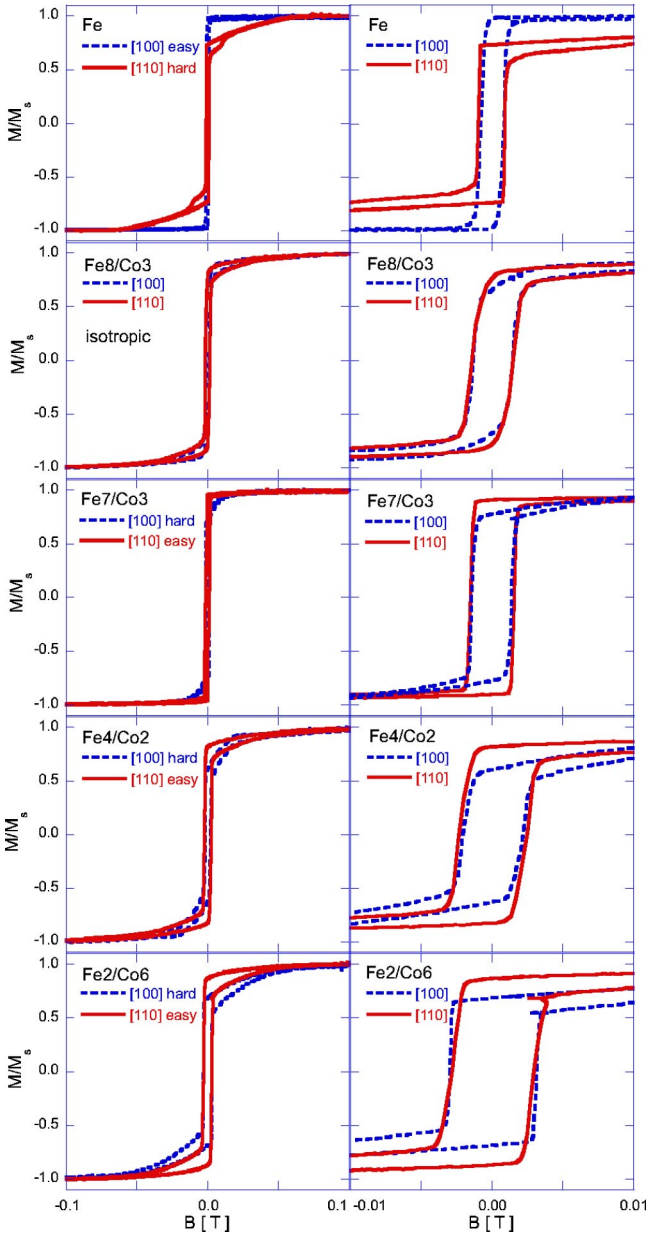

FIG. 1. The normalized magnetization vs field for Fe/Co multilayer films, $t=20$ nm. The composition is given in the figure in numbers of Fe and Co monolayers. The field was applied in the plane of the films in the crystalline directions as noted in the figure.

The saturation magnetization was determined from the slope of a linear fit of the saturation moment versus volume for all samples of each film. The uncertainty in the estimated values of M_S in our multilayers is a maximum value including the variation in the measured m_s, of the order of $\pm 1.8\%$, and the uncertainty in the determination of the film thicknesses, cf. Sec. II A. The obtained values of M_s are high (Table I), yielding effective moments $\mu_{eff}=(2.4\pm 0.2)\mu_B$, $(2.3\pm 0.1)\mu_B$, $(2.4\pm 0.4)\mu_B$, and $(2.8\pm 0.3)\mu_B$ per atom for the Fe8/Co3, Fe7/Co3, Fe4/Co2, and Fe2/Co6 multilayers, respectively. These values are in reasonable agreement with magnetization data for FeCo alloys in the same concentration range as quoted by Bozorth,[34] except for the highest

TABLE I. Magnetic parameters obtained from hysteresis curves of epitaxial bcc Fe/Co(001) multilayer films, $t=20$ nm. c is the concentration of Co. The field was applied in a crystalline direction in the plane of the film, noted as the hard (h) and easy (e) direction, respectively.

Sample	c (at. %)	K_1 kJm^{-3}	M_s kAm^{-1}	B along	B_c (mT)	M_r/M_s
Fe8/Co3	27	-3.0	1820 ± 160	[100]	1.4	0.66
				[110]	1.5	0.77
Fe7/Co3	30	-13.6	1780 ± 110	[100] h	1.6	0.69
				[110] e	1.3	0.94
Fe4/Co2	33	-30.0	1840 ± 300	[100] h	2.1	0.49
				[110] e	2.4	0.71
Fe2/Co6	75	-75.3	2150 ± 130	[100] h	3.1	0.67
				[110] e	2.8	0.87

Co concentration. The multilayer Fe2/Co6 yields a higher effective magnetic moment per atom, $(2.8\pm0.3)\mu_B$, compared to $(2.18\pm0.10)\mu_B$ for an alloy with 70% Co. The ratio between the values of the remanence obtained for the easy and hard directions, respectively, is 1.4 ± 0.1 for Fe7/Co3, Fe4/Co2, and Fe2/Co6. This is close to the value $\sqrt{2}$ expected for a film with cubic anisotropy. For each of the films the coercivity is about the same in the easy and hard directions. At the same time the coercivity increases by a factor of 2 as the Co concentration changes from 27% to 75% (Table I). The coercivity measured in a field perpendicular to the film plane is an order of magnitude higher and the remanence a factor 2 to 3 lower than the corresponding in-plane values for all the multilayers.

B. Patterned structures

1. Circular elements — low shape anisotropy

The patterning process yields particle arrays with well-defined dimensions and controlled geometry. Figure 2(a) gives an example of a three-dimensional reconstruction of an AFM image of circular particles with $d_c=200$ nm made of the Fe8/Co3 film. The corresponding MFM image is shown in Fig. 2(b). It can be concluded that the magnetic moments of each particle form a closed domain structure. For this size of the circular particles, only two-domain states were observed, independent of the magnetocrystalline anisotropy of the material. MFM images of larger circular particles ($d_c=550$ nm) made of multilayers with the lowest (Fe8/Co3) and highest (Fe2/Co6) Co content are shown in Figs. 2(c) and 2(d). The domain configuration of the circular particles made of the nearly isotropic Fe8/Co3 film consists of eight domains forming a closed structure [Fig. 2(c)], implying that the domain structure is mainly governed by the shape anisotropy. The circular particles of Fe2/Co6, with the highest magnetocrystalline anisotropy, form closed domain structures as well, now with a mainly fourfold symmetry reflecting the magnetocrystalline anisotropy of the initial film [Fig. 2(d)]. The influence of the magnetocrystalline anisotropy is evident also in the hysteresis curves of the patterned structures. This can be seen in Fig. 3 for the circular particles with $d_c=550$ nm in a field applied along the [110] direction. This direction is an easy axis in the continuous film of Fe2/Co6. The hysteresis curve of the circles made of this film is char-

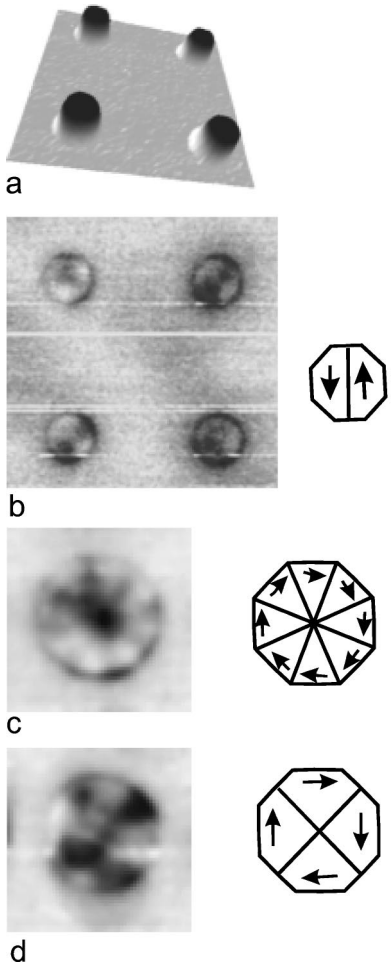

FIG. 2. Images of circular particles made of Fe/Co multilayer films, $t=20$ nm. (a) and (b) AFM and MFM images of Fe8/Co3 circles with $d_c=200$ nm. (c) and (d) MFM images of particles with $d_c=550$ nm of Fe8/Co3 and Fe2/Co6, respectively. The scan areas are 2 μm$\times$2 μm in (a) and (b) and 1 μm$\times$1 μm in (c) and (d). The sketches illustrate the proposed domain structures.

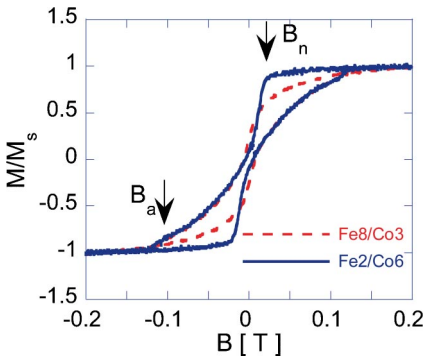

FIG. 3. The normalized magnetization vs field for circular particles with $d_c=550$ nm made of Fe8/Co3 and Fe2/Co6 multilayers, $t=20$ nm. The field was applied in the [110] direction.

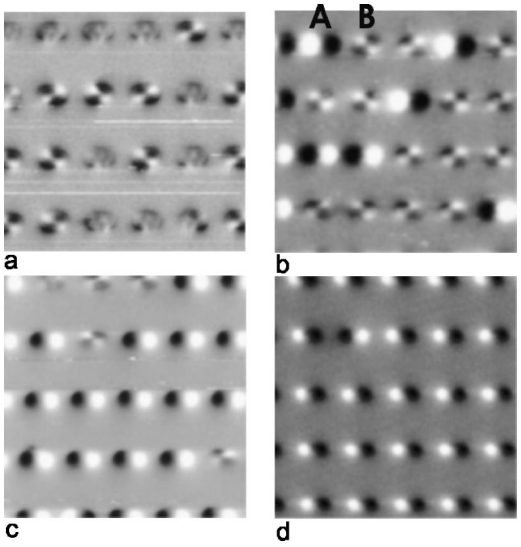

FIG. 4. MFM images of elliptical particles ($s=150$ nm, $l=450$ nm, and $t=20$ nm) positioned with their axes along the easy magnetocrystalline directions. The particles are made of (a) pure Fe, (b) Fe8/Co3, (c) Fe2/Co6, and (d) pure Co. The images were taken in zero field after ac demagnetization along the long axis. The scan areas are 5 μm$\times$5 μm.

acteristic for the processes of nucleation, motion and annihilation of domain walls.[29,30] During demagnetization, the magnetization decreases only slightly until a field $B_n \approx 25$ mT is reached. There a step in the hysteresis curve indicates the onset of nucleation of domain walls. As the field is further decreased, the magnetization drops to zero within a narrow field range. The circular particles of Fe8/Co3 have a low effective anisotropy which causes the demagnetization to initially occur by magnetization rotation, shown in the gradual decrease of magnetization, before nucleation of domain walls takes place at about 13 mT. The coercivity is slightly higher for Fe8/Co3 ($B_c=6.9$ mT) than for Fe2/Co6 ($B_c=5.2$ mT) circles, both values being higher than that of the initial films. The values of M_r/M_s are 0.10 and 0.21 for Fe2/Co6, and Fe8/Co3 respectively. In the range from B_c to negative saturation the same kind of magnetization processes occur in the circles both of Fe8/Co3 and Fe2/Co6, and the field where domain walls annihilate is $B_a \approx -112$ mT for both samples. The circular particles made of the Fe7/Co3 and Fe4/Co2 films show a behavior intermediate between the two extreme cases of high and low magnetocrystalline anisotropy.

2. Elliptical elements—varying magnetocrystalline anisotropy

When the elliptical particles are positioned with their axes along the easy directions, the magnetocrystalline and shape anisotropies cooperate. In this case the elliptical particles made of the Fe/Co multilayers were observed to have two possible zero-field domain states, comprising either one or two magnetic domains. Figure 4 shows the MFM images of the ellipses made of the Fe8/Co3 and Fe2/Co6 multilayers. For comparison MFM images of identical particles made of pure bcc Fe(001) (Ref. 35) and fcc Co(001) (Ref. 31) are included. The number NSD of single domain (SD) particles was determined as a statistic average over about 500 elements that were observed after ac demagnetization along the long axis of the ellipses. NSD is strongly influenced by the Co content, see Table II. Going from the multilayers with the lowest Co content (Fe8/Co3) to the highest (Fe2/Co6), NSD varies in the range 20–80 %. All of the particles made of pure Fe are in multidomain states, with each particle comprising either two or five domains, and all of the particles made of pure Co are single domains [Figs. 4(a) and 4(d)]. The experiments clearly demonstrate how the domain structure of the elliptical particles is developed as the magnetocrystalline anisotropy of the initial films is varied (Fig. 1). After demagnetization along the short axis the majority of the elliptical particles relax to multidomain states for all Fe/Co multilayers.

TABLE II. Magnetic parameters of elliptical particles ($s=150$ nm, $l=450$ nm, and $t=20$ nm) positioned with their axes along a crystalline direction in the Fe/Co(001) film, noted as the hard or easy magnetization direction. c is the Co concentration and NSD the relative number of SD particles observed in zero field after demagnetization along the long axis. The field B was applied along the long axis of the ellipses.

Sample film	c (at. %)	NSD %	B along	B_c (mT)	M_r/M_s
Fe8/Co3	27	29	[100]	47.6	0.54
		18	[110]	44.7	0.60
Fe7/Co3	30	12	Hard	45.6	0.72
		22	Easy	52.9	0.79
Fe4/Co2	33	33	Hard	48.8	0.49
		39	Easy	54.1	0.51
Fe2/Co6	75	31	Hard	46.3	0.79
		78	Easy	74.7	0.84

3. Elliptical elements—interplay between shape and crystalline anisotropy

By positioning the elliptical particles with their axes along the hard direction, we demonstrate how the competition between the magnetocrystalline and shape anisotropies affects the magnetic properties. As expected, for all multilayers the SD state becomes less favorable in this case. The difference between the values of NSD obtained for the two orientations is particularly significant for Fe2/Co6, the material with the highest magnetocrystalline anisotropy. This is demonstrated in Fig. 5, showing MFM images of the elliptical particles in the state after demagnetization along the long axis. When the particles have their axes parallel to the easy direction of magnetization, 78% of them are in the SD state and the others in a two-domain state [Fig. 5(a)]. For the ellipses positioned along the hard magnetocrystalline direction NSD is significantly lower, 31%. It should be noted that in this case some of the SD particles have the direction of their magnetization tilted at an angle of about 45° with respect to the long axis of the ellipses, see Fig. 5(b). Thus, the moments of these par-

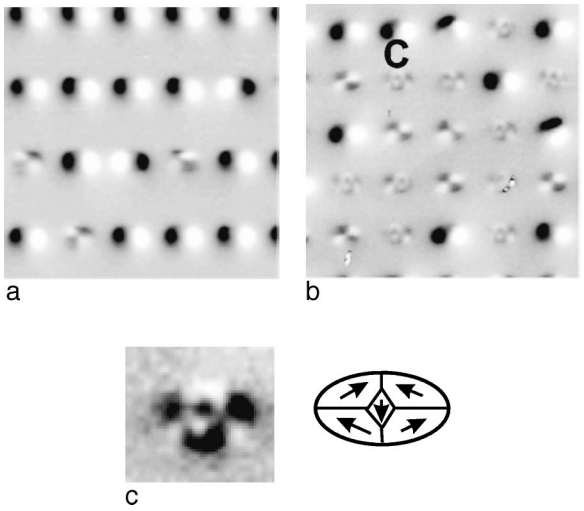

FIG. 5. MFM images of elliptical particles ($s=150$ nm, $l=450$ nm, and $t=20$ nm) made of a Fe2/Co6 multilayer film. The long axis is along the (a) easy [110] and (b) hard [100] magnetocrystalline direction of the bcc structure. The images were taken in zero field after ac demagnetization along the long axis. The scan areas are 5 μm$\times$5 μm. (c) The particle marked by C in (b) together with a sketch of its proposed domain structure.

ticles are aligned in the easy magnetocrystalline direction. Furthermore, particles with a more complex magnetic structure than only two domains appear among the ellipses. The results of this experiment are summarized in Table II.

The magnetic hysteresis curves for the field applied along the long axes of the elliptical particles are shown in Fig. 6.

The coercivity of the particles is in all cases significantly higher (15–40 times) than that of the corresponding film, and in all cases B_c is higher when the ellipses have their axes along the easy magnetocrystalline direction, see Table II. The difference becomes substantial for the case of Fe2/Co6 multilayers with the highest magnetocrystalline anisotropy. As measured with the field along the easy axis, the values of M_r/M_s for the elliptical particles are about 20% lower than that of the corresponding reference films, but after correction for demagnetizing effects in the individual particles the values become approximately equal.

For three of the investigated multilayers the elliptical particles demonstrate a characteristic step in the hysteresis curves, marked by arrows in Fig. 6. This feature appears either in both curves, as for Fe4/Co2, or only in the curve corresponding to the favorable direction of particle orientation, as for Fe8/Co3 and Fe2/Co6. The characteristic field where the step appears is $B_{st}=-2.6$, -2.6, and -3.0 mT for Fe8/Co3, Fe4/Co2, and Fe2/Co6, respectively. The hysteresis curves for the ellipses made of Fe7/Co3 are more square and the step is absent.

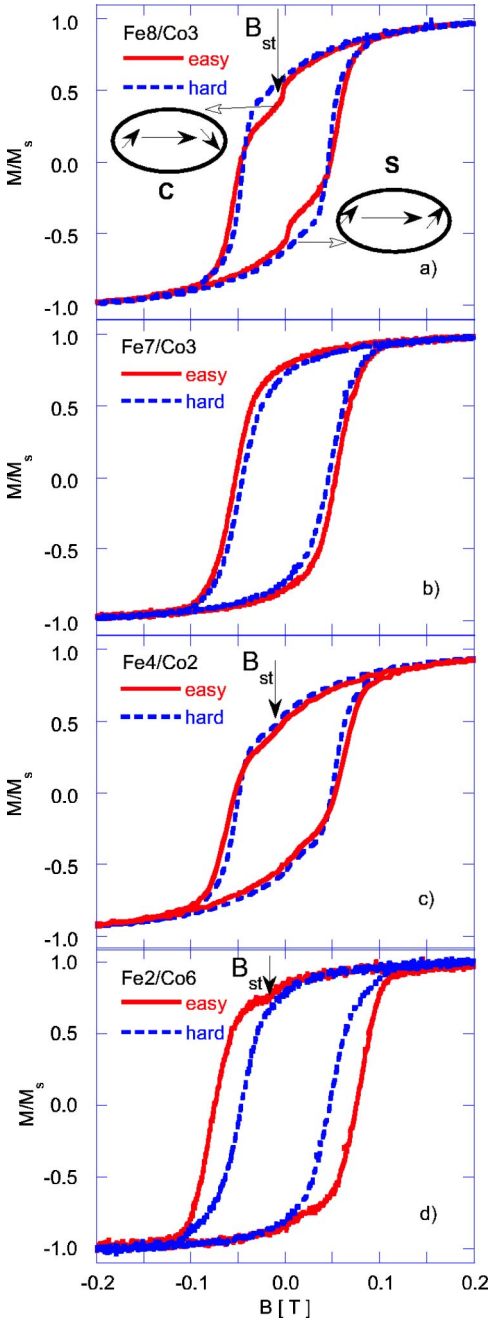

FIG. 6. The normalized magnetization vs field for elliptical particles ($s=150$ nm, $l=450$ nm, and $t=20$ nm) of Fe/Co multilayers with composition as indicated in the figure. The field was applied along the long axis of the ellipses, in the hard or easy magnetocrystalline direction of each film according to notations in the figure.

IV. DISCUSSION

A. Fe/Co films

The magnetization measurements show that all the Fe/Co multilayer films have a cubic magnetocrystalline anisotropy, with a value of K_1 depending linearly on the Co concentration. An extrapolation of the linear relation yields $K_1=0$, implying a transition of the easy axis from the initial [100] direction in Fe to [110] in Fe/Co, at about 23% Co. This agrees well with the results for similar Fe/Co multilayers with a higher number of repetitions,[19] in which the transition took place at 30% of Co. Comparing multilayers of different thickness (our data and Ref. 19) we find that the symmetry of the magnetic anisotropy in Fe/Co multilayer films is pre-

served, but the concentration at which the transition occurs is shifted towards lower Co content in the thinner films. This may be an effect of a thickness dependent magnetostrictive component leading to a higher effective anisotropy in the thinner films. The change in the distribution of the magnetocrystalline easy directions is typical also for FeCo alloys.[36] In this case a significant difference was found between the behavior of film and bulk materials: K_1 changed sign at 20% of Co for a 20 nm thick film and at 45% for the bulk material.[37] This difference could again be related to stronger magnetostrictive effects in thin films. Finally, comparing the concentration dependence of K_1 in Fe/Co multilayers (our data) and FeCo alloys of similar thickness,[37] there is only a small difference which could be attributed to the ordered arrangement of Fe and Co atoms in the material, as well as strain related to the interfaces. Thus we conclude that the change of anisotropy is a common feature in FeCo alloys and multilayers, with the concentration at which the transition occurs depending on the distribution of Fe and Co in the material and the presence of strain.

The values of the saturation magnetization of the Fe/Co multilayers are all higher than what would be obtained from the weighted bulk values of Fe and Co. Although this enhancement is compatible with the general trend of the results obtained for materials containing Fe and Co, as discussed in the Introduction, the effect is more pronounced in the multilayers containing thin individual layers of Co and Fe. The uncertainty in the estimates of M_s in our multilayers (mainly due to the uncertainty in the determined film thicknesses) does not admit a detailed analysis of the spatial distribution of moments on Fe and Co. However, we conclude that the enhancement cannot be attributed solely to the local moment of Fe. In particular, this becomes evident as we analyze the mean value $\mu_{eff}=(2.8\pm0.3)\mu_B$ per atom obtained for Fe2/Co6, the multilayer with the highest Co concentration. Assuming that the moment of Fe is $3.0\mu_B$, the highest possible value, a moment of at least $2.2\mu_B$ per Co atom is needed to explain the high average value of the multilayer. Whereas such high values were not observed in alloys, cf. the Introduction, our results agree well with magnetization measurements on other Fe/Co multilayers.[12,19] For multilayers in which the Co layers were thinner than 2.5 nm the results from magnetic hysteresis measurements were interpreted by attributing a large magnetization ($2.7\mu_B$ per atom) to interfaces comprising two Co and three Fe atomic planes[12] and retaining the bulk moments for atoms in layers further away from the interface. At the same time as the magnetization measurements imply that the Co moment should be enhanced above its bulk value, experiments probing the local moments in neutron reflectivity[19] or MCXD (Ref. 13) do not supply such evidence. This apparent contradiction might be removed if, in addition to the enhancement of the local moments of Fe and Co, one also considers a possible spin polarization of the conduction electron gas. In our multilayers showing strongly enhanced magnetization, the thicknesses of the individual Fe and Co layers are in the range 0.3–1.2 nm. In metallic systems with lateral extensions in this range, confinement and quantization phenomena may occur.[38] A condition for observations of such phenomena in multilayers is that the interfaces are sharp.

The overall magnetization reversal process for fields along (or close to) the hard magnetocrystalline direction in Fe7/Co3, Fe4/Co2, and Fe2/Co6 (Fig. 1 left column, dashed lines) can be explained as follows. As the field strength is reduced after saturation, the magnetization coherently rotates towards the nearest easy axis (the slope of the curve in the 1st quadrant). When a field of the opposite polarity is applied, at some critical point domain walls are nucleated which then sweep easily across the sample (the sharp step in the curve). Then the walls annihilate and the whole film is again uniformly magnetized but along an orthogonal easy axis. Further increase of the field strength leads to rotation of the magnetization, away from the easy axis into the direction of the applied field (slope of the curve in the 3rd quadrant). With the field applied along the easy magnetocrystalline axis in Fe7/Co3, Fe4/Co2, and Fe2/Co6 (Fig. 1 left column, solid lines), after saturation the magnetization remains practically constant until the field changes polarity and at some point domain walls nucleate. Then the magnetization jumps in two steps through domain wall propagation: first to one of the two possible orthogonal easy directions and finally to the direction of the reversing field (antiparallel to the initial easy axis). All the investigated multilayers behave as single-component systems. This confirms that the coupling between the Fe and Co layers is ferromagnetic, as also found in Ref. 39.

The coercivity increases with Co concentration, both for the easy and hard direction in the multilayers with a pronounced magnetocrystalline anisotropy: Fe7/Co3, Fe4/Co2, and Fe2/Co6. The loops of the Fe8/Co2, Fe4/Co2, and Fe2/Co6 multilayers have long hysteretic tails up to 0.05 T even for the easy direction of magnetization (Fig. 1, left column). This cannot be explained only by differences in magnetocrystalline anisotropy, but shows that irreversible magnetization processes prevail in fields above 0.01 T. We attribute the high coercivity mainly to structural defects in the films (for instance dislocations and twins), which act as pinning centers for both 90° and 180° domain walls. In Co-rich Fe/Co multilayers the number of structural defects is expected to increase due to the larger distortion of the bcc lattice. The special role of the pinning centers for the domain wall transformation and propagation is well known.[33] The high-field slopes may be explained by a small contribution from spins at the surfaces and interfaces that are harder to align than the main part of the multilayer films. This contribution, however, does not significantly influence the quality of the multilayer films. This is evidenced by the ratio between the values of the remanence obtained for the easy and hard direction being 1.4 ± 0.1 for Fe7/Co3, Fe4/Co2, and Fe2/Co6, as expected for films with cubic anisotropy.

B. Patterned structures

1. Circular elements

Decreasing the lateral dimensions of the ferromagnetic films results in a variety of domain patterns, due to the com-

petition between the different contributions to the total magnetic energy. In a nanomagnet of circular shape and low magnetocrystalline energy, there is no preferred internal direction of magnetization, and the dominant effects arise through the interplay between the exchange and magnetostatic energies. This is clearly demonstrated for the circular particles ($d_c = 550$ nm) made of the isotropic Fe8/Co3 multilayer [see Fig. 2(c)]. In the center of the particles there is a gradual change of magnetic contrast and further out, at the edges, the magnetization aligns parallel with the sides of the octagon, yielding eight magnetic domains. On the other hand, in the circular particles of Fe2/Co6 the high magnetocrystalline anisotropy of the film is prominent. In this case the interplay between the exchange and magnetocrystalline anisotropy energies leads to an arrangement of the spins in domains along the four equivalent easy directions separated by domain walls. This yields MFM images of fourfold symmetry and high contrast [Fig. 2(d)]. The fact that only two-domain states were observed in the smaller circular particles ($d_c = 200$ nm) can be explained by the cost of creating a domain wall in such a small volume being less than the magnetostatic energy of a single domain. We calculated the energy γ for formation of 180° walls in the multilayer films from the equations in Ref. 40 using the values of K_1 and M_S obtained from our measurements. The exchange constant A for a multilayer was taken as the weighted mean of the values $A = 15 \times 10^{-12}\,\mathrm{Jm}^{-1}$ for bcc Fe (Ref. 41) and $26 \times 10^{-12}\,\mathrm{Jm}^{-1}$ for bcc Co, obtained from Brillouin scattering data.[42] The obtained values of γ in the range 15–20 $\times 10^{-3}\,\mathrm{Jm}^{-2}$ yield the energy of a wall along a diameter in the easy direction of magnetization a factor about 1.5 lower than the demagnetizing energy for the circular particles with $d_c = 200$ nm. Although the procedure using the mean parameter values of the film may not be valid for a multilayer, it gives a good qualitative description of how the domain structures develop in the submicron size particles.

2. Elliptical elements

When the particles with elongated shape (ellipses with axes 150 and 450 nm) are positioned with their axes along the easy direction of magnetization, two different zero-field states are found: one comprising a single domain and another with four alternating dark and bright fields in the MFM image [see particles *A* and *B*, respectively, in Fig. 4(b)]. The latter case corresponds to two parallel but oppositely polarized magnetic dipoles separated by a 180° domain wall, thus forming a closure domain structure. Due to the shape anisotropy the formation of a SD state is more favorable in the ellipses than in the circular particles of smaller volume, and since the wall energy increases with K_1 this leads to a corresponding increase in the number of SD particles. For the material with high magnetocrystalline anisotropy, Fe2/Co6, and in the case of unfavorably positioned particles (along the hard direction) a third possible domain state was observed: five domains forming a closure structure. This state yields a very low MFM contrast due to the weaker fields leaking out [particle C in Fig. 5 (b)]. Such complex domain structures may exist in these relatively small particles because the increase of the total length of the domain walls is compensated by a decrease of the total magnetic moment aligned in the hard direction and a change of the domain wall character.

The differences between the situations when the elliptical particles are positioned with their long axes along the easy or hard magnetocrystalline directions are clearly seen also in the magnetization measurements. In particular, the hysteresis curves of the elongated particles made of three of the investigated multilayers show interesting characteristic steps [Figs. 6(a), 6(c), and 6(d)]. To explain the magnetization reversal of these particles we address the model for elements of similar sizes made of an isotropic material, described by Rave and Hubert.[43] This is close to the case of our Fe8/Co3 ellipses [Fig. 6(a)] for which the observed shape of the hysteresis curves matches well the simulations of the two quasisingle domain configurations called the *S* and *C* states.[43] These states were predicted to appear during the magnetization reversal in elongated particles with a length $l < 500$ nm, as is the case in our study. Initially during the demagnetization small edge domains, with their magnetizations making a significant angle with that of the main domain, form at the ends of the particle. Then, in the *C* state [see sketch in Fig. 6(a)] corresponding to the case with the long axis of the ellipses along the easy magnetocrystalline direction, two irreversible events can be distinguished. In the beginning, at some field B_{st} [Fig. 6(a)] the edge domains expand creating a wall between them. Thereafter the final reversal takes place. The case with ellipses positioned along the hard axis yields a hysteresis curve characteristic for the *S* state. In an isotropic material both states have similar energy, with the *C* state being marginally preferred. It should be remembered that the particles in our samples are not all identical over the array, and there may be different magnetization processes among them. The main character is, however, well described by the reversals through the *S* and *C* states. Thus we have shown that the position of ellipses along either the easy or the hard magnetization directions influences both their domain structure and magnetization reversal process.

V. SUMMARY AND CONCLUSIONS

The magnetization measurements demonstrate the change of the easy and hard magnetization directions in the plane of the film, from [100] in pure Fe to [110] in Co rich Fe/Co multilayer films. The first-order anisotropy constant K_1 is negative and depends linearly on Co concentration in our multilayers, with Co concentrations in the range 27–75 %. The change of sign of K_1 occurs at about 23% of Co, as determined by extrapolation.

The effective magnetic moments of the multilayers are high, up to $(2.8 \pm 0.3)\mu_B$ per atom for the Fe2/Co6 multilayer film. This can be explained by an enhancement of the local moments both on Fe and Co and a spin dependent polarization of the electron gas, due to confinement in the individual Fe and Co layers of thickness in the range 0.3–1.2 nm.

The magnetic domain structure of circular particles (diameter 550 nm) is mainly governed by the shape anisotropy for the nearly isotropic Fe8/Co3 multilayers and by the strong magnetocrystalline anisotropy for the Fe2/Co6 multi-

layers. The estimated energy $15–20\times10^{-3}\,\mathrm{Jm}^{-2}$ of 180° walls in the multilayers qualitatively explains why the two-domain state observed in smaller circular particles (diameter 200 nm) is preferred to the SD state.

The shape anisotropy alone is not sufficient to stabilize the SD state in the elliptical particles (150 nm×450 nm). Only when shape and strong magnetocrystalline anisotropies cooperate it leads to the formation of stable single domains in the majority (78%) of the particles in a sample.

It can be inferred from the magnetization measurements and comparison with simulations, that the elliptical particles with weak magnetocrystalline anisotropy (Fe8/Co3) form quasisingle domain states, the so called *C* and *S* states, during the magnetization reversal.

ACKNOWLEDGMENTS

The work was financially supported by the Swedish Research Council and SSF. We are grateful for a grant from the Royal Swedish Academy of Sciences. The sample patterning was performed using the facilities at the Microtechnology Center at Chalmers.

*Electronic address: olga.kazakova@npl.co.uk

[1] G.A. Prinz, Phys. Rev. Lett. **54**, 1051 (1985).
[2] B. Swinnen, J. Dekoster, J. Meersschaut, S. Demuynck, S. Cottenier, and M. Rots, J. Magn. Magn. Mater. **156**, 71 (1996).
[3] B. Swinnen, J. Meersschaut, J. Dekoster, G. Langouche, S. Cottenier, S. Demuynck, and M. Rots, Phys. Rev. Lett. **78**, 362 (1997).
[4] J. Dekoster, E. Jedryka, M. Wójcik, and G. Langouche, J. Magn. Magn. Mater. **126**, 12 (1993).
[5] B. Swinnen, J. Dekoster, G. Langouche, and M. Rots, J. Magn. Magn. Mater. **148**, 148 (1995).
[6] L. Duò, R. Bertacco, G. Isella, F. Ciccacci, and M. Richter, Phys. Rev. B **61**, 15 294 (2000).
[7] P. Blomqvist and R. Wäppling, J. Vac. Sci. Technol. A **20**, 234 (2002).
[8] L. Néel, J. Phys. Radium **15**, 225 (1954).
[9] D.I. Bardos, J. Appl. Phys. **40**, 1371 (1969).
[10] M.F. Collins and J.B. Forsyth, Philos. Mag. **8**, 401 (1963).
[11] H.H. Hamdeh, B. Fultz, and D.H. Pearson, Phys. Rev. B **39**, 11 233 (1989).
[12] Ph. Houdy, P. Boher, F. Giron, F. Pierre, C. Chappert, P. Beauvillain, K. Le Dang, P. Veillet, and E. Velu, J. Appl. Phys. **69**, 5667 (1991).
[13] S. Pizzini, A. Fontaine, E. Dartyge, C. Giorgetti, F. Baudelet, J.P. Kappler, P. Boher, and F. Giron, Phys. Rev. B **50**, 3779 (1994).
[14] B. Kalska, P. Blomquist, L. Häggstrom, and R. Wäppling, J. Magn. Magn. Mater. **226-230**, 1773 (2001).
[15] A.M.N. Niklasson, B. Johansson, and H.L. Skriver, Phys. Rev. B **59**, 6373 (1999).
[16] R.H. Victora and L.M. Falicov, Phys. Rev. B **30**, 259 (1984).
[17] J.M. MacLaren, T.C. Schulthess, W.H. Butler, R. Sutton, and M. McHenry, J. Appl. Phys. **85**, 4833 (1999).
[18] C. Paduani and J.C. Krause, J. Appl. Phys. **86**, 578 (1999).
[19] P. Blomqvist, R. Wäppling, A. Broddefalk, P. Nordblad, S.G.E. te Velthuis, and G.P. Felcher, J. Magn. Magn. Mater. **248**, 75 (2002).
[20] Y. Xie and J.A. Blackman, Phys. Rev. B **66**, 085410 (2002).
[21] K.W. Edmonds, C. Binns, S.H. Baker, M.J. Maher, S.C. Thornton, O. Tjernberg, and N.B. Brookes, J. Magn. Magn. Mater. **220**, 25 (2000).
[22] S.H. Baker, C. Binns, K.W. Edmonds, M.J. Mayer, S.C. Thornton, S. Louch, and S.S. Dhesi, J. Magn. Magn. Mater. **247**, 19 (2002).
[23] S. Landis, B. Rodmacq, B. Dieny, B. Dal'Zotto, S. Tedesco, and M. Heitzmann, Appl. Phys. Lett. **75**, 2473 (1999)
[24] R.E. Dunin-Borkowski, M.R. McCarthy, B. Kardynal, M.R. Scheinfein, D.J. Smith, and S.S.P. Parkin, J. Appl. Phys. **90**, 2899 (2001).
[25] G.A. Prinz, Science **282**, 1660 (1998).
[26] S.A. Wolf, D.D. Awschalom, R.A. Buhrman, J.M. Daughton, S. von Molnar, M.L. Roukes, A.Y. Chtchelkanova, and D.M. Treger, Science **294**, 1488 (2001).
[27] O. Kazakova, M. Hanson, P. Blomqvist, and R. Wäppling, J. Magn. Magn. Mater. **240**, 21 (2002).
[28] M. Hanson, O. Kazakova, P. Blomqvist, and R. Wäppling, J. Appl. Phys. **91**, 7044 (2002).
[29] M. Hanson, C. Johansson, B. Nilsson, P. Isberg, and R. Wäppling, J. Appl. Phys. **85**, 2793 (1999).
[30] M. Hanson, O. Kazakova, P. Blomqvist, R. Wäppling, and B. Nilsson, Phys. Rev. B **66**, 144419 (2002).
[31] O. Kazakova, M. Hanson, P. Blomqvist, and R. Wäppling, J. Appl. Phys. **90**, 2440 (2001).
[32] M. Hanson and O. Kazakova, in *Low-Dimensional Systems: Theory, Preparation, and Some Applications*, Vol. II/91 of NATO Science Series, edited by Luis M. Liz-Marzan and Michael Giersig (Kluwer Academic Publishers, Dordrecht, 2003), p. 213.
[33] A. H. Morrish, *The Physical Principles of Magnetism* (Wiley, New York, 1965).
[34] R. M. Bozorth, *Ferromagnetism* (van Nostrand, New York, 1951).
[35] M. Hanson, O. Kazakova, P. Blomqvist, and R. Wäppling (unpublished).
[36] R.C. Hall, J. Appl. Phys. **30**, 816 (1959).
[37] Th. Mühge, Th. Zeidler, Q. Wang, Ch. Morawe, N. Metoki, and H. Zabel, J. Appl. Phys. **77**, 1055 (1995).
[38] F.J. Himpsel, J.E. Ortega, G.J. Mankey, and R.F. Willis, Adv. Phys. **47**, 511 (1998).
[39] One example for thicker Fe and Co layers is given in G. Asti, M. Carbucicchio, M. Rateo, and M. Solzi, J. Magn. Magn. Mater. **196-197**, 59 (1999).
[40] A. Aharoni, *Introduction to the Theory of Ferromagnetism* (Clarendon Press, Oxford, 1996).
[41] S. Chikazumi, *Physics of Ferromagnetism*, 2nd ed. (Clarendon Press, Oxford, 1997).
[42] X. Liu, M.M. Steiner, R. Sooryakumar, G.A. Prinz, R.F.C. Farrow, and G. Harp, Phys. Rev. B **53**, 12 166 (1996).
[43] W. Rave and A. Hubert, IEEE Trans. Magn. **36**, 3886 (2000).